UV-B TOLERANT MUTANT *ARABIDOPSIS RCD1-1* EXHIBITS HIGHER PHOTOSYNTHETIC ACTIVITY AND LESS OXIDATIVE DAMAGE

LYU, G. Z. – LI, D. B. – LIU, X. L. – LI, S. S.*

Key Laboratory of Ecology and Environmental Science in Guangdong Higher Education, School of Life Science, South China Normal University, Guangzhou 510631, China

**Corresponding author*
e-mail: lishsh@scnu.edu.cn; fax: +86-20-8521-2669

(Received 23rd Apr 2019; accepted 11th Jul 2019)

Abstract. UV-B radiation has diverse biological effects on plants. The tolerance of *rcd1-1* mutant to UV-B radiation was studied in the present research. Leaves of the wild type under UV-B exhibited chlorosis, curling, and necrotic lesions, but these phenomena were not observed in the *rcd1-1* mutant. The *rcd1-1* mutant accumulated less H_2O_2 and O_2^- under UV-B radiation, and had higher activity of anti-oxidative enzymes. UV-B radiation led to accumulation of UV-B absorbing compounds as flavonoids, and anthocyanins. The *rcd1-1* mutant under UV-B radiation had higher maximum quantum efficiency of primary photochemistry and exhibited less of a decrease of effective quantum yield of photochemical energy conversion in PS II and photochemical quenching of variable chlorophyll fluorescence yield. The *rcd1-1* mutant also showed higher non-photochemical quenching, indicating that it could dissipate excess energy. The *psbA* gene were more highly expressed in the *rcd1-1* mutant, while *ANAC013* and *UNE10* genes were negatively regulated. This may explain why the mutant had a higher photosynthetic capability under UV-B radiation. It can be confirmed that the tolerant *Arabidopsis rcd1-1* mutant under UV-B radiation exhibits higher photosynthetic activity and less oxidative damage than the wild type.
Keywords: *rcd1-1 mutant, UV-B, flavonoids, anthocyanins, gene expression*

Abbreviations: Chl *a* + *b*: chlorophyll *a* and chlorophyll *b*; Fm: maximal fluorescence of a dark-adapted sample; Fo: initial fluorescence of a dark-adapted sample; Fm': maximal fluorescence of an illuminated sample; Fs: minimal fluorescence of an illuminated sample; PSI: photosystem I; PSII: photosystem II; UV-A: ultraviolet-A radiation (315–400 nm); UV-B: ultraviolet-B radiation (280–315 nm); UV-C: ultraviolet-C radiation (wavelength < 280 nm)

Introduction

Ultraviolet radiation from sunlight is divided into three spectral regions: UV-A, UV-B and UV-C. In a natural environment, plants are exposed to 10–100 times more UV-A (315–400 nm) photons than they are to UV-B (280–315 nm) photons (Verdaguer et al., 2017). UV-B radiation has received most attention because it is strongly absorbed by ozone. UV-C, with wavelength shorter than 280 nm, does not reach ground. The decrease of the ozone layer led to a significant increase in UV-B radiation from 1970 till about 1995 and shifts in the spectral UV-composition reaching the Earth surface at mid- and high latitudes. Until now little is known about the mechanism by which the *rcd1-1* mutant tolerates UV-B radiation. In the present research, we explore the UV-B resistance of the *rcd1-1* mutant by morphological and physiological properties, and gene expression. The results may explain why the mutant is tolerant to UV-B, which could enrich our understanding of the regulation mechanism of UV-B response.

http://www.aloki.hu ● ISSN 1589 1623 (Print) ● ISSN 1785 0037 (Online)
DOI: http://dx.doi.org/10.15666/aeer/1705_1181311833

Review of literature

Plants are inevitably exposed to UV-B, as they need sunlight. High doses of UV-B radiation can cause stress and damage in plant, including DNA, protein and plasma membrane damage, production and accumulation of reactive oxygen species, cell cycle arrest, chlorophyll degradation, photosynthesis inhibition, and affect various cell processes (Ulm and Jenkins, 2015; Biever and Gardner, 2016). However, UV-B not only has adverse effects on plants, but also can activate the repair mechanism in vivo, especially for plants with insufficient or no UV-B in facility culture. UV-B regulates gene expression related to physiological processes such as metabolism, morphogenesis, photosynthesis and pest resistance (Jenkins, 2014). It also regulates leaf development, regulates clock rhythm, improves plant heat tolerance, cold tolerance, drought resistance and delays flowering time (Yin and Ulm, 2017; Dotto et al., 2018).

Exposure of plants to UV-B induces photomorphogenetic as well as physiological and genetic changes, mostly injurious but sometimes beneficial. Enhanced UV-B in solar radiation could potentially induce DNA damage and radical oxygen species (ROS) production in living cells (He and Häder, 2002; Zlatev et al., 2012). On the other hand, plants have evolved a wide range of protective and repair mechanisms against UV-B stress, such as the formation of surface wax, polyamines and specific alkaloids, flavonoid biosynthesis, DNA repair and changes in metabolism (Ulm and Nagy, 2005; Fujibe et al., 2004; Frohnmeyer and Staiger, 2003). Enhanced UV-B radiation to may also result in lower photosynthesis and leads to a decrease in crop yields. Therefore, understanding how plants protect themselves against UV-B radiation is of utmost importance for agricultural production.

In recent years the model plant *Arabidopsis thaliana* has gained the much attention in research on the effects of UV, because many research tools (such as genetic, molecular biology and bioinformatics tools) could be applied to it. The intervals of *rcd1-1* on BACs F3C3 and F27G20 containing seven open reading frames were determined by genetic mapping. Six of them matched the published genome sequence of *Arabidopsis*. At1g32230 gene has a typical C-T to ethyl methylsulfonate mutation in the antisense chain, which results in G-A transition at the GT splicing site of the third exon-intron connection. RT-PCR showed that the splicing of RCD1 intron in wild type Col-0 was consistent with the predicted structure of At1g32230 and the published full-length cDNAs of CEO1 and RIKEN. In *rcd1-1*, two transcriptional types were identified by RT-PCR amplification and sequence analysis. The 2.7-kb transcript represents mRNA, in which the next (GT) in intron III downstream of the mutant shear acceptor site is used for splicing of intron III. The misspliced *rcd1-1* mRNA was only 11 bp longer than that of wild type. In *rcd1-1*, the expression level of the shorter 1.4-kb transcript was approximately the same as that of the 2.7-kb transcript. In the 1.4-kb transcript, intron splicing occurs from the 5' end of exon IV into exon III, so exon III is completely missing. Both misspliced *rcd1-1* transcript types lead to frame loss and premature termination of codons. In wild col-0, RCD1 was expressed in stem, leaf, bud and young flower, while siliques and root transcription were lower in old flower. In *rcd1-1*, compared with wild type, gene expression increased slightly, and also in old flowers and roots compared with Col-0. In siliques of *rcd1-1*, only the shorter transcripts existed at lower abundance (Ahlfors et al., 2004).

http://www.aloki.hu ● ISSN 1589 1623 (Print) ● ISSN 1785 0037 (Online)
DOI: http://dx.doi.org/10.15666/aeer/1705_1181311833

Radical-induced cell death1 (RCD1) protein is an important regulator of stress and hormonal and developmental responses in *Arabidopsis thaliana* (Jaspers et al., 2009). CEO1, also called RCD1, is a protein from *Arabidopsis thaliana* that protects yeast against oxidative damage (Belles-Boix et al., 2000; Ahlfors et al., 2004; He et al., 2012). It contains two conserved globular protein domains: the WWE domain and a poly (ADP-ribose) polymerase (PARP)-like ADP-ribose transferase catalytic domain, the former mediated by specific protein-protein interaction (Jaspers et al., 2010). When the RCD1 protein is expressed in yeast, the yeast is protected from oxidative damage induced by *tert*–butylhydroperoxide, peroxide and diamide (Belles-Boix et al., 2000). The results from gene chip research indicate that a large number of abiotic stress related genes have reduced expression in the *Arabidopsis rcd1-1* mutant (Ahlfors et al., 2004).

Thus RCD1 may be an important regulator of the oxidative stress response, and may also be involved in other abiotic stress responses in plants (Kragelund et al., 2012). This is suggested by a number of key findings. The *Arabidopsis rcd1-1* mutant has proved to be sensitive to ozone and apoplastic superoxide (Fujibe et al., 2004; Moldau et al., 2011). Forward genetic screens for ozone sensitivity and paraquat tolerance led to the isolation of *Arabidopsis rcd1-1* and *rcd1-2* mutants (Jaspers et al., 2009; Fujibe et al., 2004; Overmyer et al., 2000). The *rcd1-2* mutant is tolerant than the wild type (Fujibe et al., 2004), as is the *rcd1-1* allele (Jaspers et al., 2010; Jiang et al., 2009). The *rcd1-2* mutant is resistant to methyl viologen, and sensitive to UV-B. The *rcd1-1* mutant is sensitive to ozone and tolerant to short-term UV-B radiation. In addition, the *rcd1-1* mutant has lower sensitivity to abscisic acid, ethylene and methyl jasmonate than the wild type. Exogenous methyl ester of jasmonic acid (MeJA) inhibits the spread of cell death in *rcd1-1* mutant (Overmyer et al., 2000). By using the gene microarray technology, the expression of a large number of abiotic stress related genes were reduced in the *rcd1-1* mutant (Ahlfors et al., 2004). The *rcd1-2* mutant was resistant to a short period of UV-B radiation and exhibited higher activity of SOD and *APX* gene expression level than the wild type (Fujibe et al., 2004).

Materials and methods

Plant materials, growth conditions and UV treatment

Wild type and mutant *Arabidopsis thaliana* used in this study were all of the ecotype Columbia-0 (Col-0) background. Seeds were vernalizated at 4 °C for 3 d before sowing (Jiang et al., 2009). Seeds were surface sterilized and sown on Murashige and Skoog medium (Murashige and Skoog, 1962) containing 3% sucrose for germination and grew for 14 days under appropriate light conditions at 22 °C. White light was provided by cool white fluorescent lamps (Philips TLD30W/865 tubes, 80 W m^{-2}). Conditions for UV-B irradiation were the same as described by Jiang (Jiang et al., 2009). Radiation (hereafter referred to as UV-B) from the UV-B tubes (Philips PLS9W/01, 1.8 W m^{-2}) was filtered through cellulose acetate film (95 μm; Kunststoff-Folien-Vertrieb GmbH, Hamburg, Germany), which transmitted both UV-A and UV-B, but blocked UV-C. Radiation for control plants (hereinafter referred to as UV-A) was filtered through Mylar film, which removed both UV-B and UV-C. The spectral irradiance from the UV lamps was determined with an iHR550 spectroradiometer (HoribaJobinYvon, Japan). The spectral irradiance was weighted with the generalized plant response action spectrum, normalized to unity at 300 nm to obtain UV-B.

http://www.aloki.hu ● ISSN 1589 1623 (Print) ● ISSN 1785 0037 (Online)
DOI: http://dx.doi.org/10.15666/aeer/1705_1181311833

Root length and dry biomass

The seeds of *Arabidopsis thaliana* were planted on MS solid medium after vernalization at low temperature and surface disinfection. The culture dishes were placed vertically. The germination and seedling growth of Arabidopsis thaliana seeds were observed 2, 4, 6, 8, 10 and 12 days after sowing, and the root growth of seedlings was measured by Image J software.

Arabidopsis thaliana seedlings were harvested 14 days after sowing. The adherent MS solid medium was washed with EDTA-Na_2 and deionized water. The fresh weight was measured. Then the fresh weight was put into 65 °C oven until the constant weight, and then the dry weight was measured.

Measurement of cell membrane permeability

The membrane permeability of the wild type and *Arabidopsis rcd1* mutant was evaluated by Evans blue staining and conductivity measurement. Evans blue staining was conducted as described with some improvement. Briefly, samples were evacuated for 5 min and then infiltrated for 20 min with 0.1% Evans blue solution. The process was repeated three times, and each repetition is the average of 10 values. The samples were then boiled for 5-10 min in a mixture of 95% ethanol and lactophenol (2:1) and stored in 5% ethanol for observation. Electrical conductivity measurements were carried out with a conductivity meter (FE330, Mettler-Toledo). The first value (R1) was obtained after the clean leaves and roots were immersed in deionized water for 2 h at room temperature. After immersion for 20 min in boiling water the samples were cooled to room temperature and then measured for a second value (R2). The relative electrical conductivities were determined according to (R1/R2) × 100%.

Location of O_2^- in the leaves, location and concentration of H_2O_2 in the leaves

Generation of O_2^- in *Arabidopsis* leaves in response to UV treatment was detected by the Nitro Blue Tetrazolium (NBT) technique (Uy et al., 2011). *Arabidopsis* leaves were bathed in 0.1 mg mL^{-1} NBT solution and, following evacuation by pumping for 10 min infiltrated under dark conditions until translucent, and then placed at room temperature for 2 h. They were then boiled in 90% ethanol until the chlorophyll was completely removed. At last, the leaves were scanned and observed by Mahalingam et al. (2006). To determine H_2O_2 in the leaves, they were infiltrated as before, but with 0.3 mg mL^{-1} 2-amino benzidine (DAB) solution after UV-B treatment. They were placed in the dark for 8 h, followed by light for 2 h and then harvested and boiled in 90% ethanol until the chlorophyll was completely removed. Finally, the leaves were scanned and observed by Ma et al. (2012). H_2O_2 analysis was assayed as described by Cheeseman (2006).

Measurements of SOD, CAT and POD activity

Frozen plant leaves (1 g) were homogenized in 50 mM sodium phosphate buffer (pH 7.0) containing 0.1 mM EDTA, 0.1%(m/v) phenylmethylsulfonyl fluoride, 1% (m/v) polyvinylpyrrolidone, 0.1% (v/v) TritonX-100 and 50 mM ascorbic acid. The extract was centrifuged at 12,000 × g for 15 min and the supernatant was used for enzymatic assays. In this study, the superoxide dismutase (SOD) activity was measured by the xanthine oxidase method with SOD Activity Assay Kit (Jiancheng Bioengineering Institute, Nanjing, China). Catalase (CAT) and polyphenol oxidase (POD) activities

http://www.aloki.hu ● ISSN 1589 1623 (Print) ● ISSN 1785 0037 (Online)
DOI: http://dx.doi.org/10.15666/aeer/1705_1181311833

were measured as described by Ma et al. (2012). For SOD, the enzyme quantity that inhibits the self-oxidation rate of the reaction solution by 50% per ml under certain conditions is defined as 1 enzyme activity unit (U). For CAT, a decrease of 0.1 in A240 per minute was defined as 1 enzyme activity unit (U). For POD, a decrease of 0.01 in A470 per minute was defined as 1 enzyme activity unit (U).

Pigment, anthocyanin, flavonoid and malondialdehyde (MDA) measurements

Total chlorophyll (Chl *a* + *b)* content in plant leaves was measured by the method of Arnon (1949). The absorbance of the extract was recorded at 663 nm and 645 nm. The concentrations of chlorophyll *a*, chlorophyll *b* and total chlorophyll were calculated using the following equation:

$$\text{Chl } a = 0.0127\ \text{A663} - 0.00269\ \text{A645}$$
$$\text{Chl } b = 0.0229\ \text{A645} - 0.00468\ \text{A663}$$
$$\text{total Chl } a+b = 0.0202\ \text{A645} + 0.00802\ \text{A663}$$

Anthocyanin content was determined as described by Noh and Spalding (1998). For flavonoid measurement, 14-day old seedlings were frozen in liquid nitrogen, flavonoids were extracted and quantified as described by Kucera et al. (2003). MDA was measured with Malondialdehyde (MDA) Assay Kit (Jiancheng Bioengineering Institute, Nanjing, China) according to the manufacturer's instruction.

Photochemical activity measurements

Photochemical efficiency was evaluated from the chlorophyll *a* fluorescence of photosystem II, using a modulated fluorometer (Heinz Walz GmbH, Effeltrich, Germany) including optimal quantum yield (Fv/Fm), effective quantum yield (ΦPSII) and non-photochemical quenching (NPQ). Optimal quantum yield was defined as (Fm-Fo)/Fm, where Fm represents maximal and Fo initial fluorescence of a dark-adapted sample. Effective quantum yield is defined as (Fm'-Fs)/Fm', where Fm' represents the maximal and Fs minimal fluorescence of an illuminated sample (Sedej and Gaberščik, 2008). NPQ-values were determined according to the Stern-Volmer equation:

$$\text{NPQ} = (\text{Fm} - \text{Fm}')/\text{Fm}'$$

RNA extraction and quantitative real-time PCR

Total RNA was extracted from seedlings by using E.Z.N.A. Plant RNA Kit (Omega, USA) according to its protocol, then digested with DNAse I (Promega, USA) to eliminate genomic DNA contamination. First-strand cDNAs were synthesized from using PrimeScript 1st strand cDNA synthesis kit (Takara Biotechnology, China) according to the manufacturer's instructions.

The quantitative PCR (q-PCR) assays were performed with the ABI PRISM 7500 Real-time PCR system (Applied Biosystems, USA) using Power SYBR Green Master Mix (Applied Biosystems, USA) following the recommended conditions (50 °C for 2 min, then 95 °C for 10 min, followed by 40 cycles of 95 °C for 15 s and 60 °C for 1 min). Sepcific Primer 5.0 software was used to design the primers for the experiment (*Table 1*).

http://www.aloki.hu ● ISSN 1589 1623 (Print) ● ISSN 1785 0037 (Online)
DOI: http://dx.doi.org/10.15666/aeer/1705_1181311833

Table 1. *The nucleotide sequences of the primers used in qPCR*

No.	Gene	Primer (5'→3')
X16077.1	*18S rRNA*	F: CGTCCCTGCCCTTTGTACAC R: CGAACACTTCACCGGATCATT
NM_103021.3	*ANAC013*	F: AGGGAAGGATAGAGTCATTCATTGT R: AGTCCGTTCGCCATTAGGTG
X79898.1	*psbA*	F: GGTGCCATTATTCCTACTTCTGC R: GTTCATAAGGACCGCCGTTGT
NM_116222.3	*UNE10*	F: TTCCATCATCGCTCCTCCAG R: GTACGACCATCGCTACATGACC

The dissociation curve was used to check for the presence of a unique PCR product and the amplification curves was analyzed to estimate the primer pair efficiencies with the LinReg software (Czechowski et al., 2005). The average efficiency of all reactions on a plate (which was always > 1.95) was used in calculations. All reactions were carried out in three technical replicates. To normalize the qPCR data, a reference gene (18sRNA) was used for detecting gene expression in the wild type and the *rcd1-1* mutant (Jiang et al., 2009).

Statistical analysis

The GraphPad Prism 8 was used for statistical analysis and drawing. For comparing results of different treatments, Variance analysis is followed by a post-hoc test in order to determine pairwise differences. Differences were considered significant for $P < 0.05$.

Results

The rcd1-1 mutant is not sensitive to UV-B radiation

After growing for 8 days in white light condition, the *rcd1-1* mutant was significantly smaller than the wild type. The *rcd1-1* mutant had slower root growth (*Fig. 1a*) and accumulated less biomass (*Fig. 1b*). Also root growth was significantly inhibited (*Fig. 1c*). The ANOVA table for the data of *Figure 1c* (Two-way ANOVA, Sidak's multiple comparisons test) was displayed in *Table A1* in the *Appendix*. Under UV-B radiation, the wild type leaves showed chlorosis, curl, and necrotic lesions. However the *rcd1-1* mutant showed less changes under UV-B radiation (*Fig. 1d*).

The rcd1-1 mutant showed less cell membrane damage after UV-B exposure

Membrane permeability (Evans Blue Stain) correlated positively with duration of UV-B irradiation, and the stain of the wild type was deeper than that of the *rcd1-1* mutant (*Fig. 2a*). The electrical conductivity of the cell membrane exhibited a highly significant increase after UV-B radiation compared to the control. Although the electrical conductivity of the wild type was significantly less than that of the *rcd1-1* mutant before UV-B irradiation, it had a rising trend with increasing irradiation time, and was largest after UV-B irradiation for 6 h (*Fig. 2b*). The ANOVA table for the data of *Figure 2b* (Two-way ANOVA, Tukey's multiple comparisons test) was displayed in *Table A2*. These results indicated that the cell membrane damage of the wild type was more serious than that of the *rcd1-1* mutant after UV-B exposure.

http://www.aloki.hu ● ISSN 1589 1623 (Print) ● ISSN 1785 0037 (Online)
DOI: http://dx.doi.org/10.15666/aeer/1705_1181311833

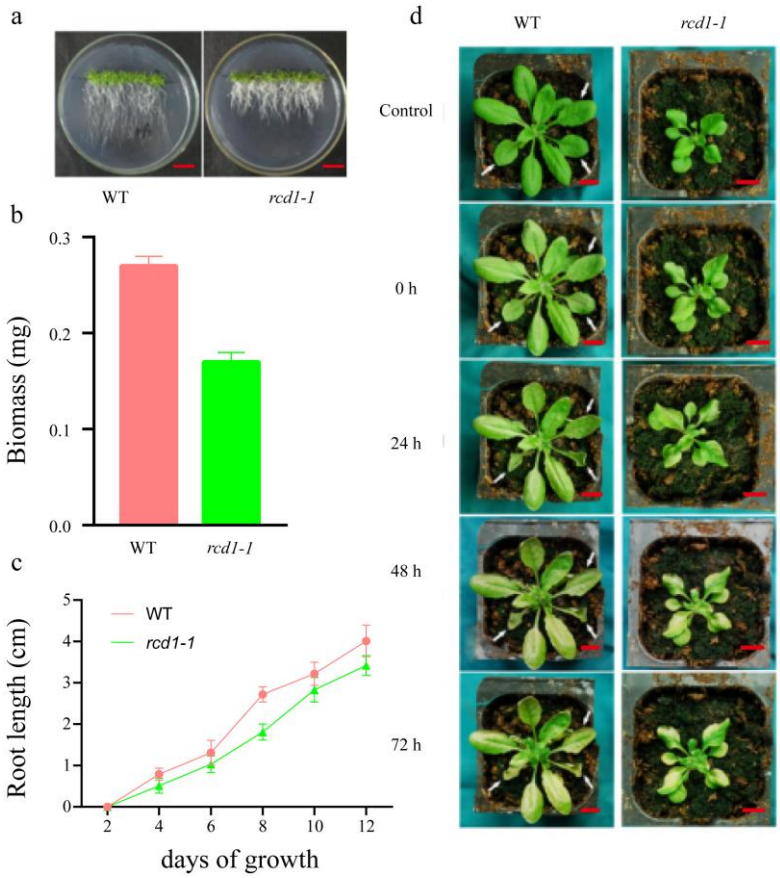

Figure 1. *The growth of Arabidopsis seedlings in normal growth condition and after UV-B radiation.* ***a*** *Seedlings of 10-day-old wild type and rcd1-1 mutant Arabidopsis.* ***b*** *Dry biomass of 10-day-old wild type and rcd1-1 mutant Arabidopsis.* ***c*** *Root length of the wild type and rcd1-1 mutant.* ***d*** *Three-week-old wild-type and rcd1-1 mutant plants were exposed to UV-B for 16 h and then allowed to recover for different time under fluorescent light before being photographed. Data are expressed as mean values ± standard errors from three replicates and error bars represent standard errors. The bar value is 10 mm*

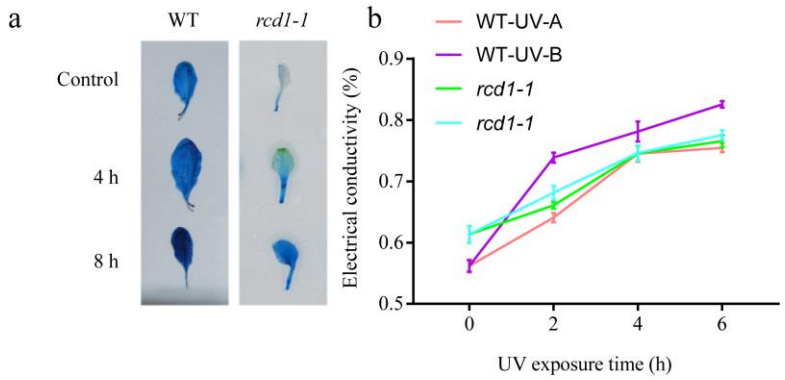

Figure 2. *Effects of enhanced UV-B radiation on cell membrane permeability of leaves. Three-week-old wild-type and rcd1-1 mutant were exposed to UV-B for 4 h and 8 h, after which the leaves were immediately harvested.* ***a*** *Leaves of the wild type and rcd1-1 mutant treated with UV-B for 0 h, 4 h and 8 h were stained with Evans blue.* ***b*** *After UV radiation, permeability of the leaves was measured with the conductivity meter. Data are expressed as mean values ± standard errors from three replicates and error bars represent standard errors*

http://www.aloki.hu ● ISSN 1589 1623 (Print) ● ISSN 1785 0037 (Online)
DOI: http://dx.doi.org/10.15666/aeer/1705_1181311833

The rcd1-1 mutant showed less content of MDA, O_2^- and H_2O_2 after UV-B exposure

To further investigate the effects of enhanced UV-B radiation on *Arabidopsis*, malondialdehyde (MDA), H_2O_2 and O_2^- productions were analyzed. The level of MDA production was significantly higher in the wild type than that in *rcd1-1* mutant after exposure for 8 h (*Fig. 3a*). The ANOVA table for the data of *Figure 3a* (Two-way ANOVA, Tukey's multiple comparisons test) was displayed in *Table A3a*. Similarly, enhanced UV-B radiation elevated H_2O_2 production considerably in the leaves after exposure for 8 h (*Fig. 3c*). The ANOVA table for the data of *Figure 3c* (Two-way ANOVA, Tukey's multiple comparisons test) was displayed in *Table A3b*. This was also shown by the DAB staining test (*Fig. 3d*). The NBT staining test showed that there was a positive correlation between accumulation of O_2^- in leaves and UV-B exposure time (*Fig. 3b*). More specifically, there was little blue precipitate in the leaves of the wild type and *rcd1-1* mutant before UV treatment and both had nearly the same light color. However, more and more blue precipitate appeared along with increasing duration of UV-B exposure, indicating that O_2^- in leaves increased. The blue precipitate in *rcd1-1* mutant leaves was less than that in the wild type at any testing time point in the whole UV-B radiation treatment process, indicating that the accumulation of O_2^- in the wild type was higher than that in *rcd1-1* mutant after UV-B radiation. In the control group (UV-A radiation treatment) the accumulation of O_2^- in the leaves was also stimulated, but the accumulation was significantly lower than for UV-B radiation. These results suggest that the damage caused by the short-term enhanced UV-B radiation to the *rcd1-1* mutant was less than that to the wild type.

Effects of antioxidant enzymatic activity of the leaves in the rcd1-1 mutant after UV-B exposure

The superoxide dismutase (SOD), peroxidase (POD) and CAT activities were assayed to investigate the effects of enhanced UV-B radiation on the antioxidative system. The SOD activity of the wild type exposed to UV-B radiation showed a slightly increasing trend, while the *rcd1-1* mutant maintained a rapid upward trend except for a decline at 4 h. The SOD activities of both genotypes were elevated after UV-B radiation for 8 h, which significantly increased from 1146 U to 1187 U in the wild type, while from 1152 U to 1299 U in *rcd1-1* mutant (*Fig. 4a*). The ANOVA table for the data of *Figure 4a* (Two-way ANOVA, Tukey's multiple comparisons test) was displayed in *Table A4a*.

The POD activity had a similar trend with the SOD activity, which showed an overall upward trend in leaves of the two genotypes with increasing duration of UV-B radiation. The difference between them was that the POD activity of *rcd1-1* mutant had always showed upward trend, while the wild type reached the highest value at the point of 6 h exposure and reduced a little at 8h. Although the POD activities of the two genotypes were almost identical under normal conditions, which increased up to 60.4% in the *rcd1-1* mutant and 41.0% in the wild type after UV-B radiation for 8 h. However, the POD enzyme activities of the two control groups treated with UV-A only increased slightly (*Fig. 4b*). The ANOVA table for the data of *Figure 4b* (Two-way ANOVA, Tukey's multiple comparisons test) was displayed in *Table A4b*.

The CAT activities differed between *rcd1-1* mutant and the wild type. The CAT activity of *rcd1-1* mutant ascended immediately under both UV-A and UV-B radiation. However, the CAT activity of the wild type fluctuated within a narrow range and finally

http://www.aloki.hu ● ISSN 1589 1623 (Print) ● ISSN 1785 0037 (Online)
DOI: http://dx.doi.org/10.15666/aeer/1705_1181311833

declined (*Fig. 4c*). The ANOVA table for the data of *Figure 4c* (Two-way ANOVA, Tukey's multiple comparisons test) was displayed in *Table A4c*. In general, the CAT activity of *rcd1-1* mutant had far higher levels than that of the wild type after UV-B radiation.

Flavonoid and anthocyanin content after UV-B exposure

As ultraviolet absorbing compounds in *Arabidopsis*, flavonoid and anthocyanin could be effectively induced when the leaves were exposed to UV-B radiation. UV exposure resulted in the accumulation of flavonoids and anthocyanin both in *rcd1-1* mutant and the wild type, but in the *rcd1-1* mutant the contents were significantly higher than in the wild type (*Fig. 5*). The ANOVA table for the data of *Figure 5b* (Two-way ANOVA, Tukey's multiple comparisons test) was displayed in *Table A5*.

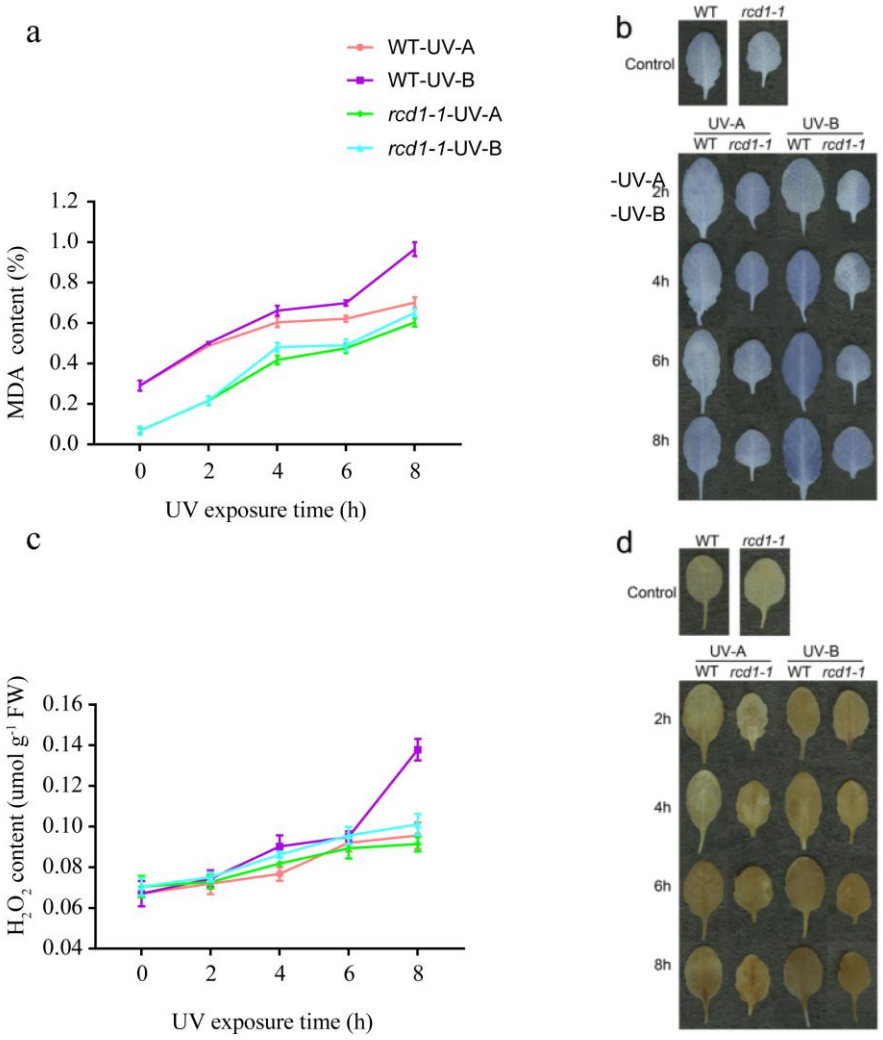

Figure 3. *Effects of enhanced UV-B radiation on the accumulation of MDA, O_2^- and H_2O_2. After UV-B radiation, the leaves were harvested.* ***a*** *MDA was measured with Malondialdehyde Assay Kit according to the manufacturer's instruction.* ***b*** *Location of O_2^- in leaves were detected by NBT staining method.* ***c*** *The concentration of H_2O_2 was measured by peroxidase coupling method.* ***d*** *Location of H_2O_2 in leaves in were detected by DAB staining method. Data are expressed as mean values ± standard errors from three replicates and error bars represent standard errors*

http://www.aloki.hu ● ISSN 1589 1623 (Print) ● ISSN 1785 0037 (Online)
DOI: http://dx.doi.org/10.15666/aeer/1705_1181311833

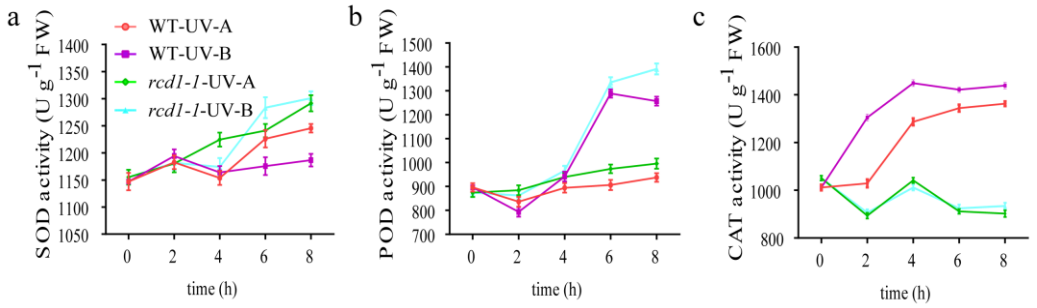

Figure 4. *Effects of enhanced UV-B radiation on the activities of antioxidant enzymes.* ***a*** *SOD;* ***b*** *POD;* ***c*** *CAT. The activity of SOD was assayed by the xanthine oxidase method, the activity of POD was detected o-methoxyphenol method and the activity of CAT was measured by spectrophotometrically. Data are expressed as mean values ± standard errors from three replicates and error bars represent standard errors*

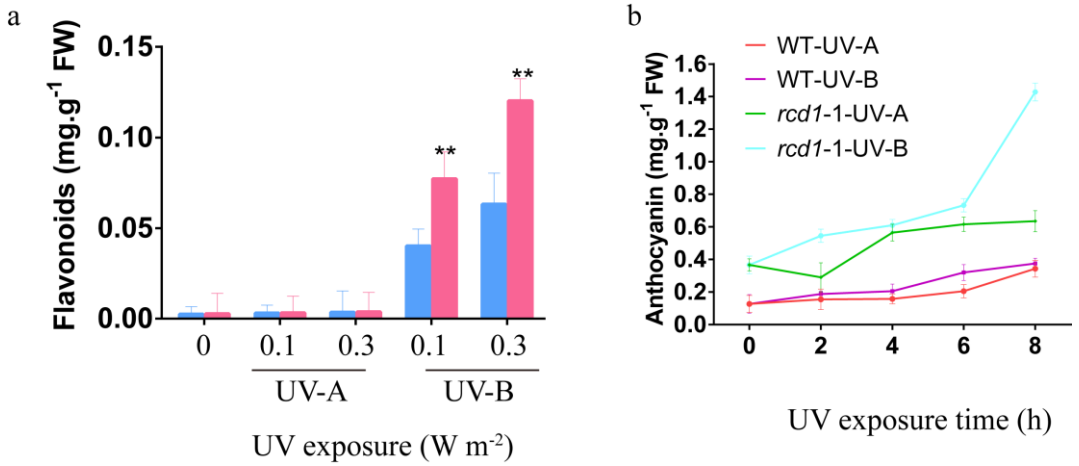

Figure 5. *Enhanced UV-B induced accumulation of UV-B absorbing compounds.* ***a*** *After UV treatment, fourteen-day-old seedlings were frozen in liquid nitrogen, flavonoids were extracted and then quantified spectrophotometrically. The symbol '*' indicates statistically differences P < 0.05 and the symbol '**'indicates statistically differences P < 0.01 (Two-way ANOVA, Tukey's multiple comparisons test).* ***b*** *Anthocyanin content in the wild type and the rcd1-1 mutant was measured spectrophotometrically. Data are expressed as mean values ± standard errors from three replicates and error bars represent standard errors*

The chlorophyll content and chlorophyll fluorescence of leaves in rcd1-1 mutant after UV-B exposure

One of the important kinds of damage of UV-B radiation to plants is the inhibition of chlorophyll synthesis. Phenotypic analysis found that the loss of green colour under UV-B radiation of the *rcd1-1* mutant was lower than that of the wild type (*Fig. 6a*). The ANOVA table for the data of *Figure 6a* (Two-way ANOVA, Tukey's multiple comparisons test) was displayed in *Table A6a*. The changes of chlorophyll content in the *rcd1-1* mutant and the wild type were measured. The downward trend of total chlorophyll in both genotypes after UV-B radiation is displayed in *Figure 6c*.

http://www.aloki.hu ● ISSN 1589 1623 (Print) ● ISSN 1785 0037 (Online)
DOI: http://dx.doi.org/10.15666/aeer/1705_1181311833

More specifically, the total chlorophyll content in both genotypes declined rapidly over the first two hours of exposure. After that, the chlorophyll content in the wild type continued to decline, while the *rcd1-1* mutant recovered transiently and chlorophyll content fell again after 8 h. After irradiation for 8 h, the total chlorophyll content in the wild type decreased by 21% while in the *rcd1-1* mutant it significantly decreased only by 15%; the total chlorophyll content of the UV-irradiated *rcd1-1* mutant was 12% higher than that of the wild type. The control group of UV-A treatment suffered only a slight decline of chlorophyll, irrespective of genotype. The trend for chlorophyll *a* was similar to that for total chlorophyll. The degradation rate of chlorophyll *a* in the wild type was significantly higher than that in *rcd1-1* mutant after UV-B radiation (*Fig. 6b*). The ANOVA table for the data of *Figure 6b* (Two-way ANOVA, Tukey's multiple comparisons test) was displayed in *Table A6b*. However, there were no differences of the degradation rate of chlorophyll *b* in the wild type and the *rcd1-1* mutant after UV-B radiation (*Fig. 6c*). The ANOVA table for the data of *Figure 6c* (Two-way ANOVA, Tukey's multiple comparisons test) was displayed in *Table A6c*.

To study the effects of enhanced UV-B radiation on photosynthesis, the chlorophyll fluorescence parameters (Fv/Fm, ϕPSII, qP and NPQ) were determined. Fluorescence values were converted to colour by chlorophyll fluorescence imager (*Fig. 7*).

The effects of enhanced UV-B radiation on the maximal efficiency of PSII photochemistry in the wild type and the *rcd1-1* mutant were reflected in the value of Fv/Fm (*Fig. 8a*). The ANOVA table for the data of *Figure 8a* (Two-way ANOVA, Tukey's multiple comparisons test) was displayed in *Table A7a*. After UV-A radiation, Fv/Fm of the wild type and *rcd1-1* mutant exhibited a slight decline -14.7% and 5% respectively. The value of Fv/Fm showed a sharp decrease from 0.79 to 0.22 (72% decrease) in the wild type under UV-B radiation, but only from 0.80 to 0.59 (26% decrease) in the *rcd1-1* mutant. The results showed that *rcd1-1* was more resistant to UV-B radiation than the wild type with respect to PSII integrity.

The quantum yield (ϕPSII) of the PSII electron transport was used to detrmine the PSII photochemical efficiency (*Fig. 8b*). The ANOVA table for the data of *Figure 8b* (Two-way ANOVA, Tukey's multiple comparisons test) was displayed in *Table A7b*. ϕPSII showed declining trends in both genotypes, but with less decline in *rcd1-1*, and none in the first two hours. Finally, ϕPSII decreased from 0.425 to 0.340 in the *rcd1-1* mutant, and from 0.420 to 0.286 in the wild type.

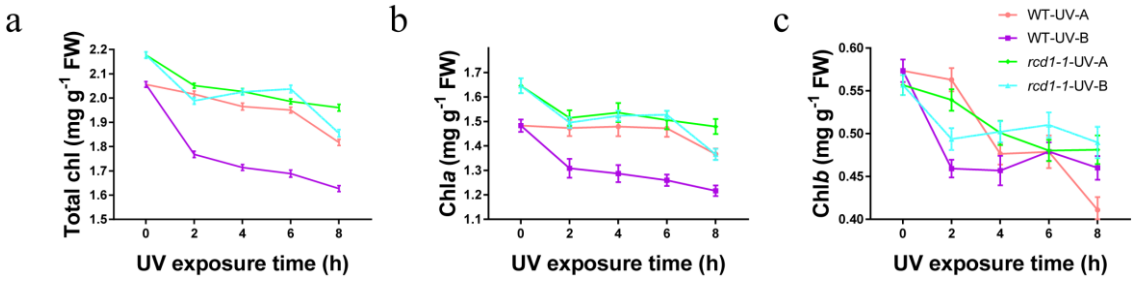

Figure 6. *Effects of enhanced UV-B radiation on chlorophyll content. After UV treatment, about 0.2 g leaves were harvested, ground in 80% (v/v) acetone solution, stored at -20 °C overnight, centrifuged and then measured OD value by spectrophotometer. Total chlorophyll content (**a**), the chl a content (**b**) and the chl b content (**c**) in the wild-type and rcd1-1 mutant were measured. Data are expressed as mean values ± standard errors from three replicates and error bars represent standard errors*

http://www.aloki.hu ● ISSN 1589 1623 (Print) ● ISSN 1785 0037 (Online)
DOI: http://dx.doi.org/10.15666/aeer/1705_1181311833

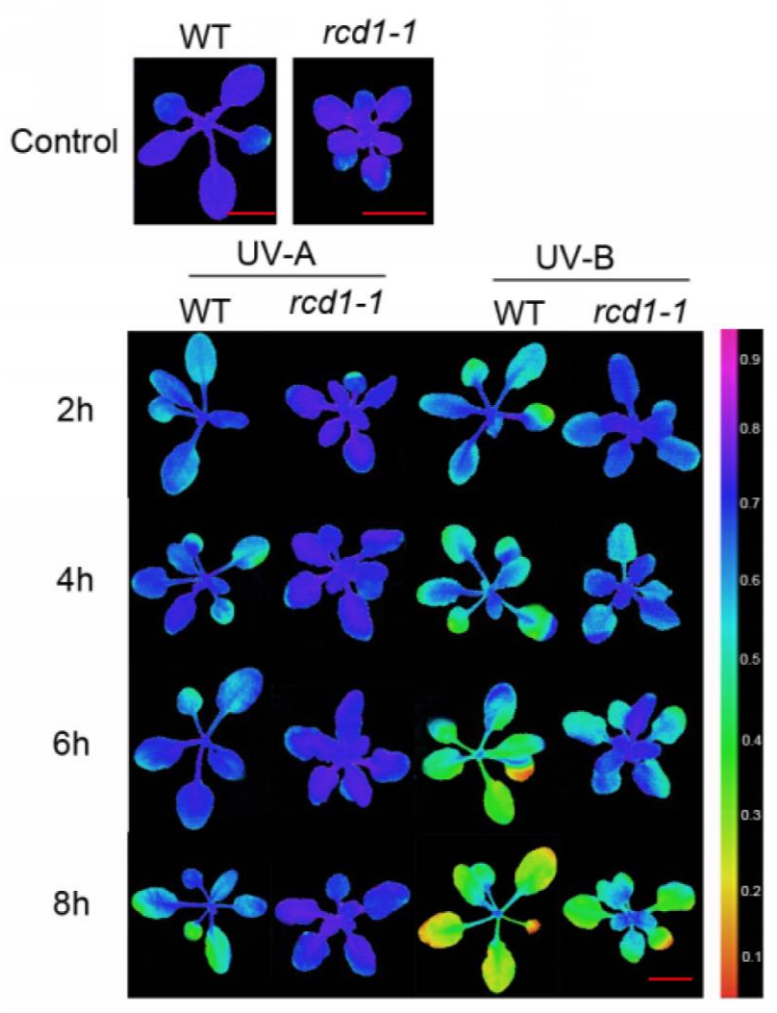

Figure 7. *Changes in fluorescence images of Fv/Fm in the wild type and rcd1-1 mutant leaves: 0 (black) to 1.0 (purple) in chlorophyll fluorescence was represented by color from black to purple. Three-week-old wild type and rcd1-1 mutants were exposed to 0.4 W m^{-2} UV for different hours and measured with Imaging-PAMM-series instrument. The bar value is 10 mm*

UV-B stress changed chlorophyll fluorescence. qP of both the wild type and *rcd1-1* mutant declined with increasing time of UV-A and UV-B exposure (*Fig. 8c*). The ANOVA table for the data of *Figure 8c* (Two-way ANOVA, Tukey's multiple comparisons test) was displayed in *Table A7c*. At the beginning of UV radiation, the qP of the wild type fell by 14.5% while that of the *rcd1-1* mutant dropped by 8%. Finally, after UV-B radiation for 8 h, the qP value of the wild type decreased by 22.6%, while that of the *rcd1-1* mutant had significantly decreased by 15%. Under normal growth condition, the non-photochemical quenching (NPQ) values of the wild type and *rcd1-1* mutant were almost the same, but at the beginning of UV-B exposure the value of NPQ of both genotypes increased slightly (*Fig. 8d*), indicating that the function of the *Arabidopsis* heat dissipation had been enhanced during this period. The ANOVA table for the data of *Figure 8d* (Two-way ANOVA, Tukey's multiple comparisons test) was displayed in *Table A7d*. After UV-B radiation for 4 h, the heat dissipation of the wild type began to decline while that of the *rcd1-1* mutant continued to rise. When plants were exposed to UV-B radiation for 6 h, the heat dissipation of the wild type was only

http://www.aloki.hu ● ISSN 1589 1623 (Print) ● ISSN 1785 0037 (Online)
DOI: http://dx.doi.org/10.15666/aeer/1705_1181311833

67.4% of that of *rcd1-1* mutant. Finally, the NPQ value decreased from 0.288 to 0.140 for the wild type, while it decreased from 0.298 to 0.193 for the *rcd1-1* mutant. The results suggested that the longer UV-B exposure impaired the PS II reaction center activity.

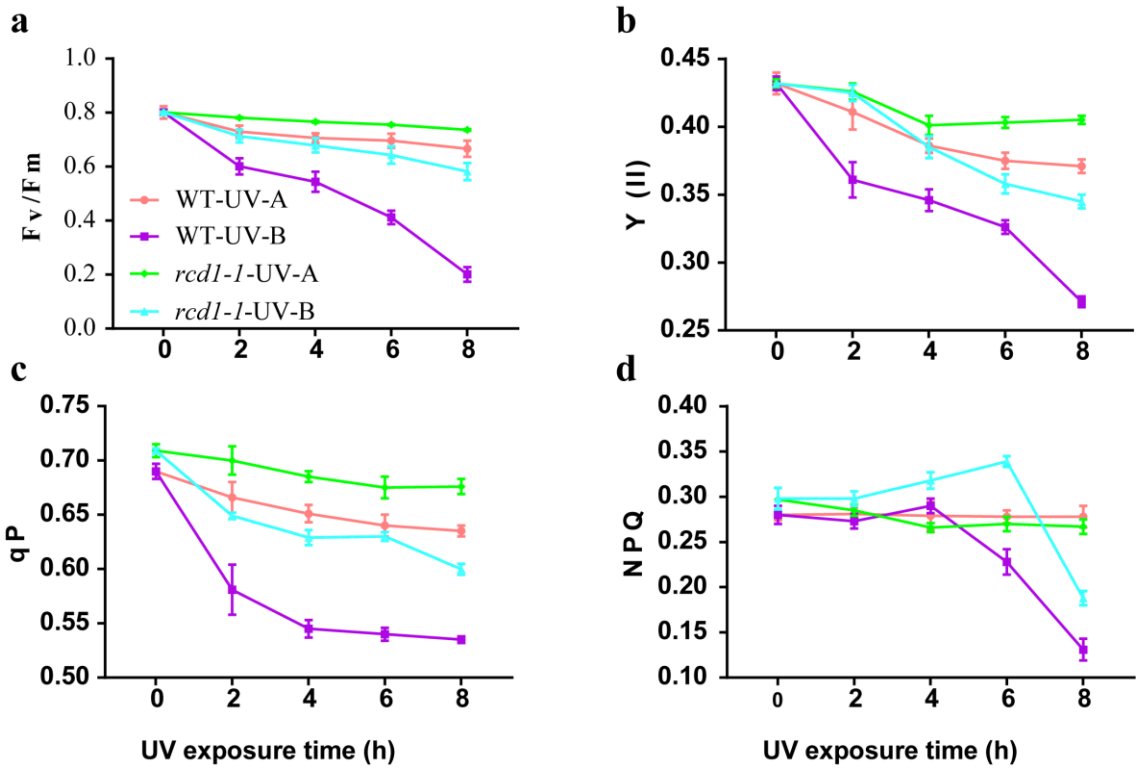

Figure 8. *Effects of enhanced UV-B radiation photosynthetic system II. After UV treatment, the maximal efficiency of PSII photochemistry (Fv/Fm)* ***(a)****, the actual PS II efficiency (ϕPSII)* ***(b)****, qP* ***(c)*** *and NPQ* ***(d)*** *of the wild type and rcd1-1 mutant were measured with Imaging-PAMM-series instrument. Data are expressed as mean values ± standard errors from three replicates and error bars represent standard errors*

Expression profile of psbA, ANAC013 and UNE10 gene in rcd1-1 mutant after UV-B exposure

Recent progress in the genetics of *Aribodopsis* has revealed that gene expression was regulated by UV-B radiation. In the present study, UV-B modulated the expression of *psbA*, *ANAC013* and *UNE10* genes at transcription level. The expression of the *psbA* gene of the photosystem II showed no consistent difference between plants of different genotypes after 6 h of UV-A treatment. The expression of *psbA* gene in *rcd1-1* mutant was higher than that in the wild type under UV-B radiation (*Fig. 9*). Although the expression of *ANAC013* gene in the two genotypes was significantly elevated both under UV-A and UV-B treatments, it was more highly expressed under UV-B treatment. On the other hand, the *ANAC013* gene was more highly expressed in the *rcd1-1* mutant than in the wild type under the same UV treatment (*Fig. 9*). The expression of the *UNE10* gene in the wild type increased under both UV-A and UV-B treatments, but most under UV-A treatment. In contrast, the expression of the *UNE10* gene in the *rcd1-1* mutant decreased under both UV-A and UV-B treatments (*Fig. 9*).

http://www.aloki.hu ● ISSN 1589 1623 (Print) ● ISSN 1785 0037 (Online)
DOI: http://dx.doi.org/10.15666/aeer/1705_1181311833

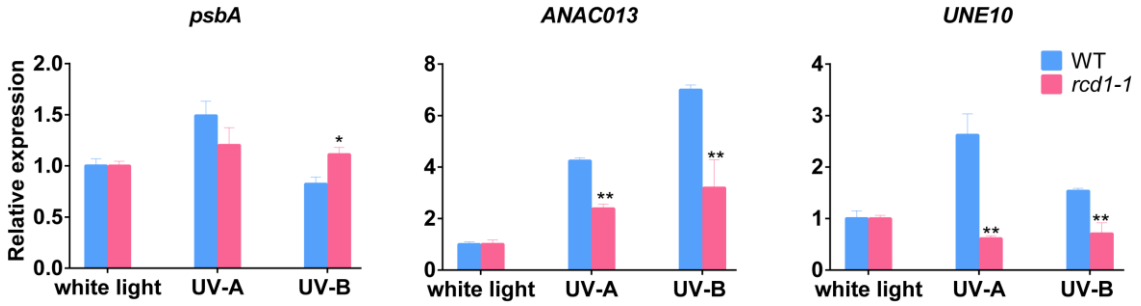

Figure 9. *UV-B-induced expression changes of light response related genes. After supplementary UV-B treatment or control UV-A treatment for 6 h, leaves of Arabidopsis wild type and rcd1-1 mutant were harvested. Relative expression of psbA, ANAC013 and UNE10 genes in the wild type and rcd1-1 mutant detected by real-time PCR. All the data shown are means ± SEM of three independent replications. Data are expressed as mean values ± standard errors from three replicates and error bars represent standard errors. The symbol '*' indicates statistically differences P < 0.05 and the symbol '**'indicates statistically differences P < 0.01 (Two-way ANOVA, Tukey's multiple comparisons test)*

Discussion

It has been reported that *rcd1-1* mutant is sensitive to ozone fumigation and apoplastic superoxide, but tolerant to methylviologen. However, the mechanisms of *rcd1-1* mutant responses to UV-B have remained to be elucidated. In the present research, we studied the effects of UV-B radiation on morphology, cellular membrane permeability, oxidative stress, antioxidant enzymatic activity, photosynthetic and sunscreen pigments, photosynthesis and photosynthetic genes expression of *Arabidopsis*. The *rcd1-1* mutant appears to be more resistant to UV-B radiation than the wild type, and the mechanism for this can now be understood.

Under ordinary growth condition, the wild type grew faster and had more biomass compared with *rcd1-1* mutant (*Fig. 1a-c*); but after UV-B radiation, the wild type exhibited chlorosis, curl, and necrotic lesions (*Fig. 1d*), while the growth of the mutant was much less affected. This was consistent with the result of changes in the chlorophyll content of leaves after UV-B radiation. Compared with the wild type, *rcd1-1* mutant showed a smaller decline in chlorophyll content when exposed to UV-B radiation (*Fig. 6*). UV-B radiation can affect the pigment concentrations in *Arabidopsis* cells by inducing photodegradation of light-absorbing pigments (Prasad and Zeeshan, 2004), resulting in loss of photosynthetic capacity. The present investigation showed that UV-B radiation significantly decreased chlorophyll *a* and *b* contents of both genotypes, but they decreased more in the wild type.

These findings prompted us to further test whether the *rcd1-1* mutant was more tolerant to UV-B radiation. The *rcd1-1* mutant suffered less serious leaf necrosis than the wild type after UV-B treatment. To further understand the extent of damage of UV-B radiation to cell membranes, the electrolyte leakage of leaves was considered, which is a classic assessment index to estimate the effects of UV-B on plasma membranes. The electrical conductivity of *rcd1-1* mutant was lower than that of the wild type after UV-B treatment. Because the higher the electrical conductivity, the more serious the injury to cell membranes; the cell membranes of *rcd1-1* mutant were less damaged than the wild type, which verified the result of Shi et al. (2005) using Evans blue staining.

http://www.aloki.hu ● ISSN 1589 1623 (Print) ● ISSN 1785 0037 (Online)
DOI: http://dx.doi.org/10.15666/aeer/1705_1181311833

Previous studies have shown that UV-B radiation induces the production of cellular reactive oxygen species (ROS), leading to oxidative stress, which in turn damages the photosynthetic apparatus (Liebel et al., 2012; Yannarelli et al., 2006). ROS accumulation induced membrane lipid peroxidation, assayed as malondialdehyde (MDA). In this present study, ROS level of the two genotypes increased in short-term enhanced UV-B treatment, revealing that UV-B radiation did induce oxidative stress. The *rcd1-1* mutant exhibited lower H_2O_2 and O_2^- accumulation levels and higher MDA level than the wild type after UV-B treatment, indicating it suffered from less oxidative stress under UV-B radiation. This might provide an explanation as to why *rcd1-1* mutant has smaller cell membrane damage than the wild type. On the other hand, antioxidant enzymes play a significant part in reactive oxygen scavenging and antioxidant defense systems. The present study showed that *rcd1-1* mutant exhibited higher activities of SOD, POD and CAT than the wild type after UV-B treatment, which explained the oxidative stress results above.

UV-B absorbing compounds, flavonoids and anthocyanin in *Arabidopsis* leaves have an important protective function reducing the transmittance of UV photons through leaf tissue (Yao and Liu, 2006). Anthocyanin production is the predominant mechanism of protection of the young plant. In the present study, *rcd1-1* mutant accumulated more flavonoids and anthocyanin than the wild type, which was similar to *rcd1-2* mutant that also accumulated more sunscreen pigments than the wild type (Ahlfors et al., 2004; Overmyer et al., 2000; Morales et al., 2015). These were evidences that *rcd1-1* mutant was more tolerant to UV-B radiation than the wild type.

Studies with artificial UV-B sources have shown that UV-B radiation may strongly affected PSII, whereas PSI appeared to be relatively insensitive (Sedej and Gaberščik, 2008). If the light energy absorbed by the plant is in excess what is needed for photosynthes, it may lead to a reduction in the potential efficiency of PSII. In the present study, *rcd1-1* mutant exhibited higher maximum quantum efficiency of primary photochemistry (Fv/Fm) than the wild type after UV-B radiation. Meanwhile, the mutant exhibited more slowly decreasing rates of effective quantum yield of photochemical energy conversion in PS II (ϕPSII) and photochemical quenching of variable chlorophyll fluorescence yield (qP). Interestingly, the *rcd1-1* mutant showed higher non-photochemical quenching (NPQ) than the wild type, so the possibility that the *rcd1-1* could release exceeded energy from UV-B by means of this process cannot be excluded. These results show that the *rcd1-1* mutant had a higher photosynthetic capability after UV-B radiation than the wild type.

RCD1 protects plant cells from running into reactive oxygen species (ROS)-triggered cell programs, including cell death, activation of pathogen-responsive genes (PR genes) and extra-plastidic antioxidant enzymes, which could support the induction of the chloroplast antioxidant system (Hiltscher et al., 2014). That the *rcd1-1* mutant exhibited higher photosynthetic capability than the wild type can be explained from the following three aspects. First, the *rcd1-1* mutant accumulated less ROS than the wild type after UV-B radiation, so its photosynthetic apparatus suffered less injury. It is known that excessive O_2^- and H_2O_2 may result in damage of PSII through their effects on the composition and structure of the light harvesting complex which lead to a disturbance in the chloroplast structure. Second, chlorophyll contents in *rcd1-1* mutant dropped less than that of the wild type after UV-B radiation. Third, the *rcd1-1* mutant had higher value of NPQ, which could release excess energy from UV-B by the process of releasing more heat than the wild type.

http://www.aloki.hu ● ISSN 1589 1623 (Print) ● ISSN 1785 0037 (Online)
DOI: http://dx.doi.org/10.15666/aeer/1705_1181311833

The two important targets of UV-B radiation in the plant are the genome and the photosynthetic machinery (Fujibe et al., 2004). One of the earliest effects of UV-B irradiation is the change of gene expression. In the present study, we have investigated changes in expression of genes of *psbA*, *ANAC013* and *UNE10*, which play important parts in photosynthesis, to further investigate the molecular mechanisms of *Arabidopsis* underlying UV-B radiation (Jaspers et al., 2009).

RCD1 is an important regulator of stress and hormonal and developmental responses in *Arabidopsis*, which might negatively regulate a wide range of stress-related down-stream genes (Jaspers et al., 2009; Fujibe et al., 2004). Previous research revealed that *RCD1* interacts with a large number of transcription factors belonging to several protein families, such as AP2/ERF, NAC and basic helix–loop–helix (bHLH) (Jaspers et al., 2009). *ANAC013* and *UNE10* belong to NAC family and basic helix–loop–helix family respectively. These results in the present research showed that *ANAC013* and *UNE10* genes are expressed to a lower extent in the mutant, which proved that *RCD1* gene negatively regulate a wide range of stress-related down-stream genes. The RCD1 functions mainly include ozone sensitivity, paraquat and UV-B tolerance and the ability to interact with different transcription factors (TFs) which could responsible for the unique functions of RCD1 (Jaspers et al., 2009). Several RCD1-interacting TFs (PIF5, PIF7, COL9, COL10 and STO) were known to play a part in light responses (Indorf et al., 2007; Castillon et al., 2007). This suggested that *RCD1* could be involved in signal transduction (Jaspers et al., 2009). *ANAC013* is regulated mainly at transcriptional level under UV-B and partly independent of *COP1*, *UVR8* and *HY5* (Jiang et al., 2012; Safrany et al., 2008). Moreover, it is also modulated by the plant hormone ABA and different abiotic stress. *UNE10* is one of light response genes and similar to *PIF7*, including MYB and BHLH domain, which play an important role in the signal path of the UV-B (Paila et al., 2008). RCD1 interacts in vivo and suppresses the activity of the transcription factors ANAC013 and ANAC017, which mediate a ROS-related retrograde signal originating from mitochondrial complex III (Shapiguzov et al., 2019). Inactivation of RCD1 leads to increased expression of mitochondrial dysfunction stimulon (MDS) genes regulated by ANAC013 and ANAC017.

The *psbA* gene is located in the chloroplast genome and encodes for the D1 protein, a core component of Photosystem II. The results in the present study revealed that the *psbA* gene of photosynthetic system II was expressed to a greater degree in *rcd1-1* mutant than the wild type, which meant photosystem II suffered less damage under UV-B. The result was in accordance with the phenomenon that the photosynthetic capability of the mutant was higher than that of the wild type. Therefore, the *RCD1* gene could be an important genetic resource to improve plant function against UV-B radiation, which may be an interested topic to provide an incentive for further scientific contributions in the near future.

Conclusion

The present research revealed that RCD-1 is sensitive to UV-B radiation in *Arabidopsis.* The *rcd1-1* mutant is more resistant to UV-B probably because of higher flavonoids and anthocyanins in the mutants. *RCD-1* gene may negatively regulate the expression of *ANAC013* and *UNE10*. More work is needed to explore the molecular mechanism of *RCD1*-mediated response to UV-B regulation.

http://www.aloki.hu ● ISSN 1589 1623 (Print) ● ISSN 1785 0037 (Online)
DOI: http://dx.doi.org/10.15666/aeer/1705_1181311833

Acknowledgements. We sincerely thank Professor Lars Olof Björn from Lund University, Sweden for his great help and critical suggestions on the research. This work was supported by the National Natural Science Foundation of China (grant NO. 31670266), the Leading Scientists Project of Guangdong Province, the Guangdong Pearl River Scholar Funded Scheme (2012), the Natural Science Foundation of Guangdong Province (grant No. 2017A030313115) and the Innovation Project of Graduate School of South China Normal University (grant NO. 2016lkxm10). We are extremely grateful to Prof. Paul Giller, School of Biological, Earth and Environmental Sciences, University College Cork, Ireland for editing the English of the manuscript. Shaoshan Li designed the research; Xianla Liu performed the experiment; Guizhen Lyu and Dongbing Li drafted the manuscript; Guizhen Lyu, Dongbing Li and Shaoshan Li read and approved the final manuscript. Conflict of interests. The authors state no conflict of interests.

REFERENCES

[1] Ahlfors, R., Lang, S., Overmyer, K., Jaspers, P., Brosch, M., Tauriainen, A. A., Kollist, H., Tuominen, H., Bellesboix, E., Piippo, M. (2004): *Arabidopsis* RADICAL-INDUCED CELL DEATH1 belongs to the WWE protein–protein interaction domain protein family and modulates abscisic acid, ethylene, and methyl jasmonate responses. – The Plant Cell 16: 1925-1937.

[2] Arnon, D. I. (1949): Copper enzymes in isolated chloroplasts, polyphenoxidase in Beta vulgaris. – Plant Physiology 24: 1-15.

[3] Belles-Boix, E., Babiychuk, E., van Montagu, M., Inze, D., Kushnir, S. (2000): CEO1, a new protein from *Arabidopsis thaliana*, protects yeast against oxidative damage. – FEBS Letters 482: 19-24.

[4] Biever, J. J., Gardner, G. (2016): The relationship between multiple UV-B perception mechanisms and DNA repair pathways in plants. – Environmental and Experimental Botany 124: 89-99.

[5] Castillon, A., Shen, H., Huq, E. (2007): Phytochrome interacting factors: central players in phytochrome-mediated light signaling networks. – Trends in Plant Science 12: 514-521.

[6] Cheeseman, J. M. (2006): Hydrogen peroxide concentrations in leaves under natural conditions. – Journal of Experimental Botany 57: 2435-2444.

[7] Czechowski, T., Stitt, M., Altmann, T., Udvardi, M. K., Scheible, W. (2005): Genome-wide identification and testing of superior reference genes for transcript normalization in *Arabidopsis*. – Plant Physiology 139: 5-17.

[8] Dotto, M., G Mez, M. S., Soto, M. S., Casati, P. (2018): UV-B radiation delays flowering time through changes in the PRC2 complex activity and miR156 levels in Arabidopsis thaliana. – Plant, Cell, Environment 41: 1394-1406.

[9] Frohnmeyer, H., Staiger, D. (2003): Ultraviolet-B radiation-mediated responses in plants. balancing damage and protection. – Plant Physiology 133: 1420-1428.

[10] Fujibe, T., Saji, H., Arakawa, K., Yabe, N., Takeuchi, Y., Yamamoto, K. T. (2004): A methyl viologen-resistant mutant of *Arabidopsis*, which is allelic to ozone-sensitive rcd1, is tolerant to supplemental ultraviolet-B irradiation. – Plant Physiology 134: 275-285.

[11] He, F., Tsuda, K., Takahashi, M., Kuwasako, K., Terada, T., Shirouzu, M., Watanabe, S., Kigawa, T., Kobayashi, N., Guntert, P. (2012): Structural insight into the interaction of ADP-ribose with the PARP WWE domains. – FEBS Letters 586: 3858-3864.

[12] He, Y., H Der, D. (2002): UV-B-induced formation of reactive oxygen species and oxidative damage of the cyanobacterium *Anabaena sp.*: protective effects of ascorbic acid and N-acetyl-l-cysteine. – Journal of Photochemistry and Photobiology B-biology 66: 115-124.

[13] Hiltscher, H., Rudnik, R., Shaikhali, J., Heiber, I., Mellenthin, M., Duarte, I. M., Schuster, G. N., Kahmann, U., Baier, M. (2014): The radical induced cell death protein 1 (RCD1) supports transcriptional activation of genes for chloroplast antioxidant enzymes. – Frontiers in Plant Science 5: 475-475.

http://www.aloki.hu ● ISSN 1589 1623 (Print) ● ISSN 1785 0037 (Online)
DOI: http://dx.doi.org/10.15666/aeer/1705_1181311833

[14] Indorf, M., Cordero, J., Neuhaus, G., Rodriguezfranco, M. (2007): Salt tolerance (STO), a stress-related protein, has a major role in light signalling. – Plant Journal 51: 563-574.
[15] Jaspers, P., Blomster, T., Brosch, M., Salojarvi, J., Ahlfors, R., Vainonen, J. P., Reddy, R. A., Immink, R. G. H., Angenent, G. C., Turck, F. (2009): Unequally redundant RCD1 and SRO1 mediate stress and developmental responses and interact with transcription factors. – Plant Journal 60: 268-279.
[16] Jaspers, P., Brosch, M., Overmyer, K., Kangasjarvi, J. (2010): The transcription factor interacting protein RCD1 contains a novel conserved domain. – Plant Signaling, Behavior 5: 78-80.
[17] Jenkins, G. I. (2014): Structure and function of the UV-B photoreceptor UVR8. – Current Opinion in Structural Biology 29: 52-57.
[18] Jiang, L., Wang, Y., Björn, L. O., Li, S. (2009): *Arabidopsis* RADICAL-INDUCED CELL DEATH1 is involved in UV-B signaling. – Photochemical and Photobiological Sciences 8: 838-846.
[19] Jiang, L., Wang, Y., Li, Q., Björn, L. O., He, J., Li, S. (2012): Arabidopsis STO/BBX24 negatively regulates UV-B signaling by interacting with COP1 and repressing HY5 transcriptional activity. – Cell Research 22: 1046-1057.
[20] Kragelund, B. B., Jensen, M. K., Skriver, K. (2012): Order by disorder in plant signaling. – Trends in Plant Science 17: 625-632.
[21] Kucera, B., Leubnermetzger, G., Wellmann, E. (2003): Distinct ultraviolet-signaling pathways in bean leaves. DNA damage is associated with β-1,3-glucanase gene induction, but not with flavonoid formation. – Plant Physiology 133: 1445-1452.
[22] Liebel, F., Kaur, S., Ruvolo, E., Kollias, N., Southall, M. (2012): Irradiation of skin with visible light induces reactive oxygen species and matrix-degrading enzymes. – Journal of Investigative Dermatology 132: 1901-1907.
[23] Ma, B., Gao, L., Zhang, H., Cui, J., Shen, Z. (2012): Aluminum-induced oxidative stress and changes in antioxidant defenses in the roots of rice varieties differing in Al tolerance. – Plant Cell Reports 31: 687-696.
[24] Mahalingam, R., Jambunathan, N., Gunjan, S., Faustin, E., Weng, H., Ayoubi, P. (2006): Analysis of oxidative signalling induced by ozone in *Arabidopsis* thaliana. – Plant Cell and Environment 29: 1357-1371.
[25] Moldau, H., Vahisalu, T., Kollist, H. (2011): Rapid stomatal closure triggered by a short ozone pulse is followed by reopening to overshooting values. – Plant Signaling & Behavior 6: 311-313.
[26] Morales, L. O., Brosche, M., Vainonen, J. P., Sipari, N., Lindfors, A., Strid, A., Aphalo, P. J. (2015): Are solar UV-B- and UV-A-dependent gene expression and metabolite accumulation in Arabidopsis mediated by the stress response regulator RADICAL-INDUCED CELL DEATH1? – Plant Cell and Environment 38: 878-891.
[27] Murashige, T., Skoog, F. (1962): A revised medium for rapid growth and bio assays with tobacco tissue cultures. – Physiologia Plantarum 15: 473-497.
[28] Noh, B., Spalding, E. P. (1998): Anion Channels and the Stimulation of Anthocyanin Accumulation by Blue Light in *Arabidopsis* Seedlings. – Plant Physiology 116: 503-509.
[29] Overmyer, K., Tuominen, H., Kettunen, R., Betz, C., Langebartels, C., Sandermann, H., Kangasjarvi, J. (2000): Ozone-sensitive *Arabidopsis* rcd1 mutant reveals opposite roles for ethylene and jasmonate signaling pathways in regulating superoxide-dependent cell death. – The Plant Cell 12: 1849-1862.
[30] Paila, U., Kondam, R., Ranjan, A. (2008): Genome bias influences amino acid choices: analysis of amino acid substitution and re-compilation of substitution matrices exclusive to an AT-biased genome. – Nucleic Acids Research 36: 6664-6675.
[31] Prasad, S. M., Zeeshan, M. (2004): Effect of UV-B and monocrotophos, singly and in combination, on photosynthetic activity and growth of non-heterocystous cyanobacterium *Plectonema boryanum*. – Environmental and Experimental Botany 52: 175-184.

http://www.aloki.hu ● ISSN 1589 1623 (Print) ● ISSN 1785 0037 (Online)
DOI: http://dx.doi.org/10.15666/aeer/1705_1181311833

[32] Safrany, J., Haasz, V., Mate, Z., Ciolfi, A., Feher, B., Oravecz, A., Stec, A., Dallmann, G., Morelli, G., Ulm, R. (2008): Identification of a novel CIS-regulatory element for UV-B-induced transcription in *Arabidopsis*. – Plant Journal 54: 402-414.
[33] Sedej, T. T., Gaberščik, A. (2008): The effects of enhanced UV-B radiation on physiological activity and growth of Norway spruce planted outdoors over 5 years. – Trees-Structure and Function 22: 423-435.
[34] Shapiguzov, A., Vainonen, J. P., Hunter, K., Tossavainen, H., Tiwari, A., Jarvi, S., Hellman, M., Aarabi, F., Alseekh, S., Wybouw, B. (2019): *Arabidopsis* RCD1 coordinates chloroplast and mitochondrial functions through interaction with ANAC transcription factors. – eLife 8: e43284.
[35] Shi, S., Wang, G., Wang, Y., Zhang, L., Zhang, L. (2005): Protective effect of nitric oxide against oxidative stress under ultraviolet-B radiation. – Nitric Oxide 13: 1-9.
[36] Ulm, R., Jenkins, G. I. (2015): Q&A: How do plants sense and respond to UV-B radiation? – BMC Biology 13: 45-50.
[37] Ulm, R., Nagy, F. (2005): Signalling and gene regulation in response to ultraviolet light. – Current Opinion in Plant Biology 8: 477-482.
[38] Uy, B., Mcglashan, S. R., Shaikh, S. (2011): Measurement of reactive oxygen species in the culture media using acridan lumigen PS-3 assay. – Journal of Biomolecular Techniques 22: 95-107.
[39] Verdaguer, D., Jansen, M. A. K., Llorens, L., Morales, L. O., Neugart, S. (2017): UV-A radiation effects on higher plants: Exploring the known unknown. – Plant Science 255: 72-81.
[40] Yannarelli, G. G., Noriega, G. O., Batlle, A., Tomaro, M. L. (2006): Heme oxygenase up-regulation in ultraviolet-B irradiated soybean plants involves reactive oxygen species. – Planta 224: 1154-1162.
[41] Yao, X., Liu, Q. (2006): Changes in morphological, photosynthetic and physiological responses of Mono Maple seedlings to enhanced UV-B and to nitrogen addition. – Plant Growth Regulation 50: 165-177.
[42] Yin, R., Ulm, R. (2017): How plants cope with UV-B: from perception to response. – Current Opinion in Plant Biology 37: 42-48.
[43] Zlatev, Z., Lidon, F. C., Kaimakanova, M. (2012): Plant physiological responses to UV-B radiation. – Emirates Journal of Food and Agriculture 24: 481-501.

APPENDIX

Table A1. *ANOVA table for the data of Figure 1c (two-way ANOVA, Sidak's multiple comparisons test)*

ANOVA table	SS	DF	MS	F (DFn, DFd)	P value
Interaction	0.7270	5	0.1454	F (5, 24) = 81.87	P < 0.0001
Row factor	62.06	5	12.41	F (5, 24) = 6989	P < 0.0001
Column factor	1.501	1	1.501	F (1, 24) = 845.0	P < 0.0001
Residual	0.04262	24	0.001776		

Table A2. *ANOVA table for the data of Figure 2b (two-way ANOVA, Tukey's multiple comparisons test)*

ANOVA table	SS	DF	MS	F (DFn, DFd)	P value
Interaction	0.01963	9	0.002181	F (9, 32) = 6.436	P < 0.0001
Row factor	0.2691	3	0.08971	F (3, 32) = 264.7	P < 0.0001
Column factor	0.01614	3	0.005381	F (3, 32) = 15.88	P < 0.0001
Residual	0.01085	32	0.0003389		

http://www.aloki.hu ● ISSN 1589 1623 (Print) ● ISSN 1785 0037 (Online)
DOI: http://dx.doi.org/10.15666/aeer/1705_1181311833

Table A3. *ANOVA table for the data of Figure 3 (two-way ANOVA, Tukey's multiple comparisons test).* ***a*** *ANOVA table for the data of Figure 3a.* ***b*** *ANOVA table for the data of Figure 3c*

(a)

ANOVA table	SS	DF	MS	F (DFn, DFd)	P value
Interaction	0.09175	12	0.007646	F (12, 40) = 5.299	P < 0.0001
Row factor	2.170	4	0.5425	F (4, 40) = 376.0	P < 0.0001
Column factor	0.7387	3	0.2462	F (3, 40) = 170.6	P < 0.0001
Residual	0.05772	40	0.001443		

(b)

ANOVA table	SS	DF	MS	F (DFn, DFd)	P value
Interaction	0.003056	12	0.0002547	F (12, 40) = 4.154	P = 0.0003
Row factor	0.01108	4	0.002771	F (4, 40) = 45.21	P < 0.0001
Column factor	0.001442	3	0.0004806	F (3, 40) = 7.841	P = 0.0003
Residual	0.002452	40	6.130e-005		

Table A4. *ANOVA table for the data of Figure 4 (two-way ANOVA, Tukey's multiple comparisons test).* ***a*** *ANOVA table for the data of Figure 4a.* ***b*** *ANOVA table for the data of Figure 4b.* ***c*** *ANOVA table for the data of Figure 4c*

(a)

ANOVA table	SS	DF	MS	F (DFn, DFd)	P value
Interaction	29590	12	2466	F (12, 40) = 12.24	P < 0.0001
Row factor	86828	4	21707	F (4, 40) = 107.7	P < 0.0001
Column factor	22413	3	7471	F (3, 40) = 37.07	P < 0.0001
Residual	8061	40	201.5		

(b)

ANOVA table	SS	DF	MS	F (DFn, DFd)	P value
Interaction	511109	12	42592	F (12, 40) = 111.4	P < 0.0001
Row factor	934451	4	233613	F (4, 40) = 611.0	P < 0.0001
Column factor	354056	3	118019	F (3, 40) = 308.7	P < 0.0001
Residual	15293	40	382.3		

(c)

ANOVA table	SS	DF	MS	F (DFn, DFd)	P value
Interaction	604397	12	50366	F (12, 40) = 294.5	P < 0.0001
Row factor	284652	4	71163	F (4, 40) = 416.1	P < 0.0001
Column factor	1485984	3	495328	F (3, 40) = 2896	P < 0.0001
Residual	6841	40	171.0		

Table A5. *ANOVA table for the data of Figure 5b (two-way ANOVA, Tukey's multiple comparisons test)*

ANOVA table	SS	DF	MS	F (DFn, DFd)	P value
Interaction	1.007	12	0.08394	F (12, 40) = 33.73	P < 0.0001
Row factor	1.502	4	0.3756	F (4, 40) = 151.0	P < 0.0001
Column factor	2.798	3	0.9328	F (3, 40) = 374.9	P < 0.0001
Residual	0.09953	40	0.002488		

http://www.aloki.hu ● ISSN 1589 1623 (Print) ● ISSN 1785 0037 (Online)
DOI: http://dx.doi.org/10.15666/aeer/1705_1181311833

Table A6. *ANOVA table for the data of Figure 6 (two-way ANOVA, Tukey's multiple comparisons test).* ***a*** *ANOVA table for the data of Figure 6a.* ***b*** *ANOVA table for the data of Figure 6b.* ***c*** *ANOVA table for the data of Figure 6c*

(a)

ANOVA table	SS	DF	MS	F (DFn, DFd)	P value
Interaction	0.1097	12	0.009143	F (12, 40) = 18.28	P < 0.0001
Row factor	0.5708	4	0.1427	F (4, 40) = 285.3	P < 0.0001
Column factor	0.6734	3	0.2245	F (3, 40) = 448.9	P < 0.0001
Residual	0.02000	40	0.0005001		

(b)

ANOVA table	SS	DF	MS	F (DFn, DFd)	P value
Interaction	0.06287	12	0.005239	F (12, 40) = 1.970	P = 0.0542
Row factor	0.2621	4	0.06552	F (4, 40) = 24.64	P < 0.0001
Column factor	0.4580	3	0.1527	F (3, 40) = 57.40	P < 0.0001
Residual	0.1064	40	0.002659		

(c)

ANOVA table	SS	DF	MS	F (DFn, DFd)	P value
Interaction	0.06287	12	0.002607	F (12, 40) = 4.434	P = 0.0002
Row factor	0.2621	4	0.01916	F (4, 40) = 32.59	P < 0.0001
Column factor	0.4580	3	0.02172	F (3, 40) = 3.694	P = 0.0194
Residual	0.1064	40	0.0005879		

Table A7. *ANOVA table for the data of Figure 8 (two-way ANOVA, Tukey's multiple comparisons test).* ***a*** *ANOVA table for the data of Figure 8a.* ***b*** *ANOVA table for the data of Figure 8b.* ***c*** *ANOVA table for the data of Figure 8c.* ***d*** *ANOVA table for the data of Figure 8d*

(a)

ANOVA table	SS	DF	MS	F (DFn, DFd)	P value
Interaction	0.2876	12	0.02396	F (12, 40) = 16.21	P < 0.0001
Row factor	0.4283	4	0.1071	F (4, 40) = 72.45	P < 0.0001
Column factor	0.5588	3	0.1863	F (3, 40) = 126.0	P < 0.0001
Residual	0.05912	40	0.001478		

(b)

ANOVA table	SS	DF	MS	F (DFn, DFd)	P value
Interaction	0.01670	12	0.001392	F (12, 40) = 10.10	P < 0.0001
Row factor	0.05295	4	0.01324	F (4, 40) = 96.12	P < 0.0001
Column factor	0.03519	3	0.01173	F (3, 40) = 85.18	P < 0.0001
Residual	0.005509	40	0.0001377		

(c)

ANOVA table	SS	DF	MS	F (DFn, DFd)	P value
Interaction	0.02015	12	0.001679	F (12, 40) = 7.184	P < 0.0001
Row factor	0.05911	4	0.01478	F (4, 40) = 63.23	P < 0.0001
Column factor	0.09733	3	0.03244	F (3, 40) = 138.8	P < 0.0001
Residual	0.009348	40	0.0002337		

(d)

ANOVA table	SS	DF	MS	F (DFn, DFd)	P value
Interaction	0.04849	12	0.004041	F (12, 40) = 16.25	P < 0.0001
Row factor	0.04648	4	0.01162	F (4, 40) = 46.72	P < 0.0001
Column factor	0.02003	3	0.006676	F (3, 40) = 26.85	P < 0.0001
Residual	0.009948	40	0.0002487		

http://www.aloki.hu ● ISSN 1589 1623 (Print) ● ISSN 1785 0037 (Online)
DOI: http://dx.doi.org/10.15666/aeer/1705_1181311833